Innovative Food Science and Emerging Technologies 102 (2025) 104004

Contents lists available at ScienceDirect

Innovative Food Science and Emerging Technologies

journal homepage: www.elsevier.com/locate/ifset

Structure and functional properties of myosin induced by electrostatic fields at different pH values

Yuqian Xu [a,b,1], Dongmei Leng [a], Martine Schroyen [b], Xin Li [a], Debao Wang [a], Dequan Zhang [a], Chengli Hou [a,*]

[a] Institute of Food Science and Technology, Chinese Academy of Agricultural Sciences, Key Laboratory of Agro-Products Quality and Safety Control in Storage and Transport Process, Ministry of Agriculture and Rural Affairs, Beijing 100193, PR China
[b] Precision Livestock and Nutrition Unit, Gembloux Agro-Bio Tech, University of Liège, Passage de Déportés 2, Gembloux, Belgium

ARTICLE INFO

Keywords:
Electrostatic field
Myosin
pH value
Protein structure
Protein function

ABSTRACT

In this study, the effects of electrostatic field on myosin structure and function at different pH values were investigated. The results demonstrated that a higher surface hydrophobicity and lower sulfhydryl group content of the electrostatic field (EF) group compared to Control group ($P < 0.05$). The particle size, secondary structure, and microstructure investigations revealed that the EF group had decreased protein aggregation and a more stable protein structure. Furthermore, the application of electrostatic field improved the water holding capacity (WHC) of myosin gel by enhancing interaction between water molecules and protein, reducing the loss of free and immobilized water. In addition, the structure of the gel formed by electrostatic field was more stable, showing higher gel hardness and dense microstructure. The study further revealed that the internal mechanism of electrostatic field to maintain the quality of fresh meat may be related to maintaining the structural and functional activity of myosin.

1. Introduction

There is a dynamic variation of pH value in postmortem muscles, which inevitably leads to modifications in the muscle protein (Liu, Oey, et al., 2018). According to studies, protein in its native state often carries a negative charge and is comparatively stable close to the isoelectric point (pI) (Han et al., 2022; Sun et al., 2024). However, alterations in charged groups and electrostatic interactions between proteins could be impacted by external and internal variation pH value conditions, thus altering protein structure and function. As reported by Yu, Chen, et al. (2024), Yu, Hong, et al. (2024), Yu, Yan, et al. (2024), pH value alters the distribution of electrostatic charges on the protein surface, which in turn affects the structure of the protein. Other investigations have also confirmed that the change of hydrogen bond stability triggers the weakening of protein interaction, which ultimately leads to the loss of α-helix (Zhang et al., 2024). Therefore, exploring new technologies with high effective value to adjust the distribution of charge on the protein surface, maintaining the structure and function of protein in different pH value conditions, and ultimately promoting its better function is a crucial aspect of improving meat quality.

Previous studies have shown the positive methods that reduce the degradation of proteins at different pH values, such as the addition of non-meat proteins, including proline (Zhou & Yang, 2020), lard-based diacylglycerol, or egg white proteins (Walayat et al., 2020; Zhao et al., 2020). Additionally, the external techniques, including pulsed ultrasonic treatment (Sun et al., 2021) and low and high pressure processing (Chen et al., 2023; Guo et al., 2019) have been successfully applied to mitigated the destruction of protein structure and characteristics. Electrostatic field has been demonstrated as a promising non-thermal method for maintaining the storage quality of fresh meat (Xie et al., 2023). Different from the technologies mentioned above, the electrostatic field does not bring other additional substances to affect the sense of the material, nor does it cause a cavitation effect to damage the material structure. It has the advantages of efficiency of energy transfer and less energy consumption in applications, which was make it attractive to researchers and entrepreneurs in the preservation field (Wang et al.,

* Corresponding author at: Institute of Food Science and Technology, Chinese Academy of Agricultural Sciences, No. 2 Yuanmingyuan West Road, Haidian District, Beijing 100193, PR China.
E-mail address: houchengli@caas.cn (C. Hou).
[1] Institute of Food Science and Technology, Chinese Academy of Agricultural Sciences, No.2 Yuanmingyuan West Road, Haidian District, Beijing, 100,193, P. R. China

https://doi.org/10.1016/j.ifset.2025.104004
Received 30 December 2024; Received in revised form 24 February 2025; Accepted 11 March 2025
Available online 14 March 2025

2018). Studies have shown that the charge released by the electrostatic field has a positive effect on the electrostatic interaction between macromolecular substances and the adjustment of the surface net charge distribution (Rodrigues et al., 2019; Xie et al., 2023). Proteins, as macromolecular substances, exhibit substantial surface charge densities that constitute a fundamental mechanism underlying the role of electrostatic fields in maintaining their structural and functional integrity (Pereira et al., 2024). This phenomenon has been substantiated by Rodrigues et al. (2020), who proposed that while protein biological functions are closely associated with their structural conformations, external electrostatic fields may induce conformational modifications through electrostatic interactions. In general, the electrostatic field exerts multifaceted effects on the meat protein system, mainly through the electrostatic shielding effect to maintain the structure, delay oxidation, and mitigate protein denaturation and aggregation. Furthermore, the modification of charge distribution collectively strengthens protein and water interactions through optimized hydrogen bonding networks and electrostatic attraction forces, ultimately enhancing the functional properties of the protein. Xie, Chen, et al. (2021), Xie, Zhou, et al. (2021) demonstrated that external electrostatic fields mitigate protein oxidative damage through a dual mechanism involving charge release and modulation of interprotein electrostatic forces. Also, Rodrigues et al. (2019) demonstrated that the regulation of protein surface potentials and intermolecular interactions by electrostatic fields provides a controllable strategy for charge redistribution and optimization of functional protein properties. Additionally, some researchers suggested that electrostatic fields could inhibit protein oxidation and preserve structural integrity by facilitating directional charge arrangement (Qian et al., 2019). Similarly, based on our earlier research, we found that electrostatic field influences the process of actomyosin combination and dissociation by released charges, regulates the contraction and relaxation of muscle fibers, and ultimately regulates the degree of muscle tenderization during the postmortem (Xu et al., 2024). Numerous studies have investigated the effects of electrostatic fields on water molecule dynamics. Electrostatic fields optimize ice crystal formation through charge-mediated nucleation control, thereby regulating water migration in meat and enhancing muscle WHC (Lin et al., 2025; Wang et al., 2024; Xie, Chen, et al., 2021,Xie, Zhou, et al., 2021). Research on the effects of electrostatic fields on the integrity and function of muscle proteins remains limited, with most studies focusing on whole meat treatment rather than independent investigations of proteins in meat. Considering the strong association between electrostatic interactions and the structural and functional properties of proteins, it is reasonable to hypothesize that electrostatic fields exert a positive effect on proteins (Rodrigues et al., 2020). This approach may be regarded as a promising technique for maintaining the structural integrity of protein at different pH value conditions.

Therefore, the following experiments were conducted for this study: myosin was selected as the target protein to establish myosin models at 4 different pH value conditions (9.0, 7.0, 5.0, 3.0), due to it is the main component of the myofibrillar lattice (Xie et al., 2023). The changes of secondary structure, microstructure, oxidation properties, texture properties and thermal processing properties of myosin with and without the application of an electrostatic field were comprehensively analyzed. This study attempts to explain how the electrostatic field maintains the integrity of myosin at different pH values from the perspective of maintaining the structure and function of protein, thereby enhancing the storage quality of meat. We supposed that this work could contribute to a better comprehension of the potential principle of the function of electrostatic fields in the preservation of meat and put forward a fresh insight into the preservation of meat.

2. Materials and methods

2.1. Materials

2.1.1. The preparation of myosin solution

Myosin was obtained by purifying commercial myosin isolates (M1636, SIGMA-ALDRICH, SHANGHAI, CHINA). Purity and conformation meet the requirements. Myosin protein solution (MYPs) of 10 % *v*/v, 10 mg protein/mL was prepared by preparing 50 mmol/L K_3PO_4 buffer (3 mmol/L Na_3PO_4) with pH of 9.0, 7.0, 5.0, and 3.0. The solution was stirred for 2 h to ensure that it was completely dissolved, and then checked the pH value. The pH values of the MYPs measured at 25 ± 0.5 °C were 9.0, 7.0, 5.0, and 3.0, respectively. And adjust the pH value with hydrochloric acid or sodium hydroxide if needed.

2.1.2. The treatment of electrostatic field

10 mL volume of MYPs was placed in a 90 mm disposable plate (after ultraviolet disinfection), and the solution was stationary for 10 min to make the surface of the solution stable. Then, MYPs were treated at −1 ± 0.2 °C under 12 kV electrostatic field for 6 h, the parameters of the procedure were selected from our previous studies (Xu et al., 2024). The distance between the solution surface and the discharge plate of electrostatic field was 5 ± 0.2 cm. MYPs treated without electrostatic field were used as the Control group, and those treated with electrostatic field were used as the EF group. After the treatment, the sample was collected and transferred to a glass tube and equilibrated at 4 °C for 24 h.

2.1.3. The preparation of the MYPs samples

The MYPs powder was prepared by vacuum freeze-drying (LGJ-10, BEIJING FOUR-RING SCIENCE INSTRUMENT PLANT LTD., BEIJING, CHINA) to evaluate the protein secondary structure (FTIR) and microstructure (SEM). After pre-freezing at −20 °C for 2 h, freeze-drying temperature was −65 °C for 24 h and pressure was 15 MPa. The obtained protein powder sample was immediately transferred to −80 °C for storage and named myosin protein solution powder (MYPp). The remaining MYPs samples were used to determine surface hydrophobicity, sulfhydryl group content (-SH), protein Zeta-potential and particle size distribution, protein degradation degree (SDS-PAGE), and fluorescence spectrum. MYPs gel was prepared by MYPs after heating and its WHC (T_2 relaxation time, H - proton content, and centrifugal loss), texture profile analysis (TPA), and microstructure were determined.

2.2. Surface hydrophobicity

The 1 mL of 2 mg/mL MYPs was homogenized with 40 μL of 1 mg/mL bromophenol blue solution, followed by incubation under 25 ± 0.5 °C for 15 min. The MYPs were centrifuged at 3000 ×*g* for 15 min, 4 °C. The supernatant was taken and measured at 595 nm. (A_2) Take 1 mL of 20 mmol/L phosphate buffer (0.6 mol/L NaCl, pH 6.5) instead of MYPs as the Control group (A_1). Characterize the surface hydrophobicity with the connection volume of bromophenol blue.

$$\text{MYPs surface hydrophobicity } (\mu g) = (A_1 - A_2)/A_1 \times 40$$

Where, 40 is the volume of bromophenol blue.

2.3. Sulfhydryl group contents

According to the method of Liu et al. (2023), 5 mL of urea-triglycine buffer (pH 8.0) and 0.02 mL of 5,5′ - dithiobis-2-nitrobenzoic acid reagent (4 mg/mL) were combined with 0.5 mL of MYPs. The mixes were measured at 412 nm following a 30-min dark incubation period at 25 ± 0.5 °C.

$$-\text{SH}(\mu\text{mol/g protein}) = 73.53 \times A_{412} \times D/C$$

Where, A_{412} is the absorbance at a wavelength of 412 nm; D is the dilution factor (6.04); C is the sample concentration (mg/mL); and -SH is the total quantity of sulfhydryl group (μmol/g).

2.4. Zeta-potential and particle size distribution

The determination procedure referred to Xu et al. (2024), briefly, the 1 mL of 1 mg/mL MYPs suspension was loaded in a machine. Zeta-potential and particle size distribution of MYPS was measured by a Zeta Potential Analyzer (NANO ZS90, MALVERN INSTRUMENTS LTD., UK).

2.5. SDS-page

SDS-PAGE was performed by previously method (Chen et al., 2023): The same volume of loading buffer was mixed with 1 mg/mL MYPs, which were then heated for 5 min in boiling water. Each sample (5 μL) was added to a gel containing 4 % concentrate and 12 % separation. It was initially operated at 80 V and then run at 120 V. The 0.1 % (*w/v*) Coomassie Blue R250 was used to stain the gel overnight, decolorized with decolorizing solution at 25 ± 0.5 °C until clear bands appeared, and finally observed in Bio-Rad imaging system (BIO-RAD, HERCULES, CALIFORNIA, USA).

2.6. Fluorescence spectrum

The procedure was carried out according to Deng et al. (2025) with minor modification, the 0.2 mg/mL MYPs were collected to measure the fluorescence spectrum (HITACHI F-4600, SHIMADZU, JAPAN). Excitation wavelength: 283 nm. The emission light was obtained at 300–400 nm. Scan speed: 1000 nm/min.

2.7. Secondary structure components

Received MYPp 1 mg from 2.1.3. The secondary structure components of MYPp were monitored with an FTIR spectrophotometer (TENSOR 27 FTIR, BURUKER, IMMANUELSHOFEN, BADEN-WURTTEMBERG, GERMANY). FTIR spectra were scanned and recorded at 500–4000 cm^{-1}. Plot after recording fixed values. The Amide *I* region could primarily be associated with the overlapping bands, including α-helix (1646–1664 cm^{-1}), random coil (1637–1645 cm^{-1}), β-sheet (1664–1681 cm^{-1}), and β-turn (1615–1637 and 1682–1700 cm^{-1}).

2.8. Preparation of MYPs gel

The MYPs gel was prepared according to the study of Xu et al. (2023). The MYPs were collected and put into a closed glass bottle, then it was heated from 25 °C to 80 °C within 55 min, and kept heated at 80 °C for 30 min. After the end of the time, it was cooled in ice water to 25 ± 0.5 °C, and stored at 4 °C overnight to determine the following indexes.

2.9. Water holding capacity (WHC)

The T_2 relaxation time and H-proton density of the gel were measured referred to the method of Xu et al. (2023) with minor modifications. The 2.0 ± 0.05 g gel was placed in a tube for determination. The main parameters of T_2 include: Proton resonance frequency 20 MHz, TW (ms) = 4500, TE (ms) = 0.5, NS = 4, NECH = 18,000. The main parameters of H-proton density include: repetition time of 2000 MS, performing 4 repetition times, longitudinal relaxation time of 20 MS, and spin echo time of 20 MS.

The centrifugal loss was also according to Xu et al. (2023) with some modification. The 2.00 ± 0.05 *g* protein gel was centrifuged at 8000 ×*g* at 4 °C for 10 min, and the residual moisture was removed after centrifugation. The centrifugal loss (%) was expressed as the percentage of the mass of the gel after centrifugation relative to that before centrifugation.

2.10. Texture profile analysis (TPA)

The gel was cut into cylinders with a diameter of 2 cm and a height of 2 cm and placed in a glass tube. The P/0.5 probe (Diameter: 0.5 mm) of the texture analyzer (TA-XT PLUS®, STABLE MICRO SYSTEM, UK) was selected to determine the TPA. The pre-measurement rate of 2 mm/s, the mid-measurement rate of 1 mm/s, and the post-measurement rate of 1 mm/s, the pressing distance was 4 mm of the gel height, initiating force was 5 g.

2.11. Scanning electron microscopy (SEM)

MYPp was obtained from 2.1.3 and fixed on the observation platform with gold. The morphology of the MYPp was evaluated by SEM (SU8010, HITACHI, JAPAN). The images were obtained at the magnification of 1000 × .

The sample was cut from the central area of the gel and vacuum freeze-dried. The morphology of the MYPs was evaluated by the same SEM machine. All images were obtained at the magnification of 2000×.

2.12. Statistical analysis

The overall test was carried out twice, and the indicators in each test were repeated for 3 times, and the data were expressed as mean ± SE. One-way ANOVA was analyzed using SPSS Statistics 26.0 software and Duncan's method to determine the significance between the data ($P < 0.05$). Origin 2021 was used to produce the figures.

3. Results and discussion

3.1. Surface hydrophobicity and sulfhydryl group contents of MYPs

It was observed that the surface hydrophobicity of MYPs was lowest at pH 7.0 and reached a maximum at pH 9.0 (Fig. 1b). Zhang et al. (2019) proposed the same conclusion that the surface hydrophobicity of pH value was the lowest near the pI. Changes in pH value altered the molecular flexibility and structure of the protein, resulting in an enhanced exposure of hydrophobic groups on the surface of protein subunits (Yu, Chen, et al., 2024; Yu, Hong, et al., 2024; Yu, Yan, et al., 2024). The surface hydrophobicity was higher at pH 3.0 and 9.0, and proteins were substantially more hydrophobic in alkaline environments than in acidic ones, which might be attributed to the alkaline impact might led to an expansion of protein molecules, causing the interaction of hydrophobic groups that related to the protein assemble (Liu et al., 2024). Moreover, the surface hydrophobicity of the EF group was lower than that of the Control group at pH 7.0 and 5.0, suggesting that the electrostatic fields had a great influence on the solubility, ionization, and charge characteristics of proteins (Liu, Oey, et al., 2018; Liu, Wei, et al., 2018). The large and tiny molecule fragments, peptides, and amino acids were common forms of proteins under electrostatic fields that were not favorable for the exposure and formation of hydrophobic groups, resulting in a decline in the surface hydrophobicity of the protein and an enhancement in dispersion, which was consistent with the research conclusions of Liu, Wei, et al. (2018) and Zhou et al. (2015).

As shown in Fig. 1c, the contents of sulfhydryl groups in both groups were significantly lower than pH 7.0 under acidic and alkaline conditions ($P < 0.05$). The electrostatic field treated protein sulfhydryl group had a larger concentration than the other two groups at pH 9.0 and 5.0 ($P < 0.05$). The myosin molecule consists of about 42 hydrophobic groups, including sulfur amino acids, cysteine, and methionine with high oxidation sensitivity were altered in the process of protein oxidation (Walayat et al., 2024). It was known that these sulfhydryl groups were easily oxidized to generate disulfide bonds, which might promote

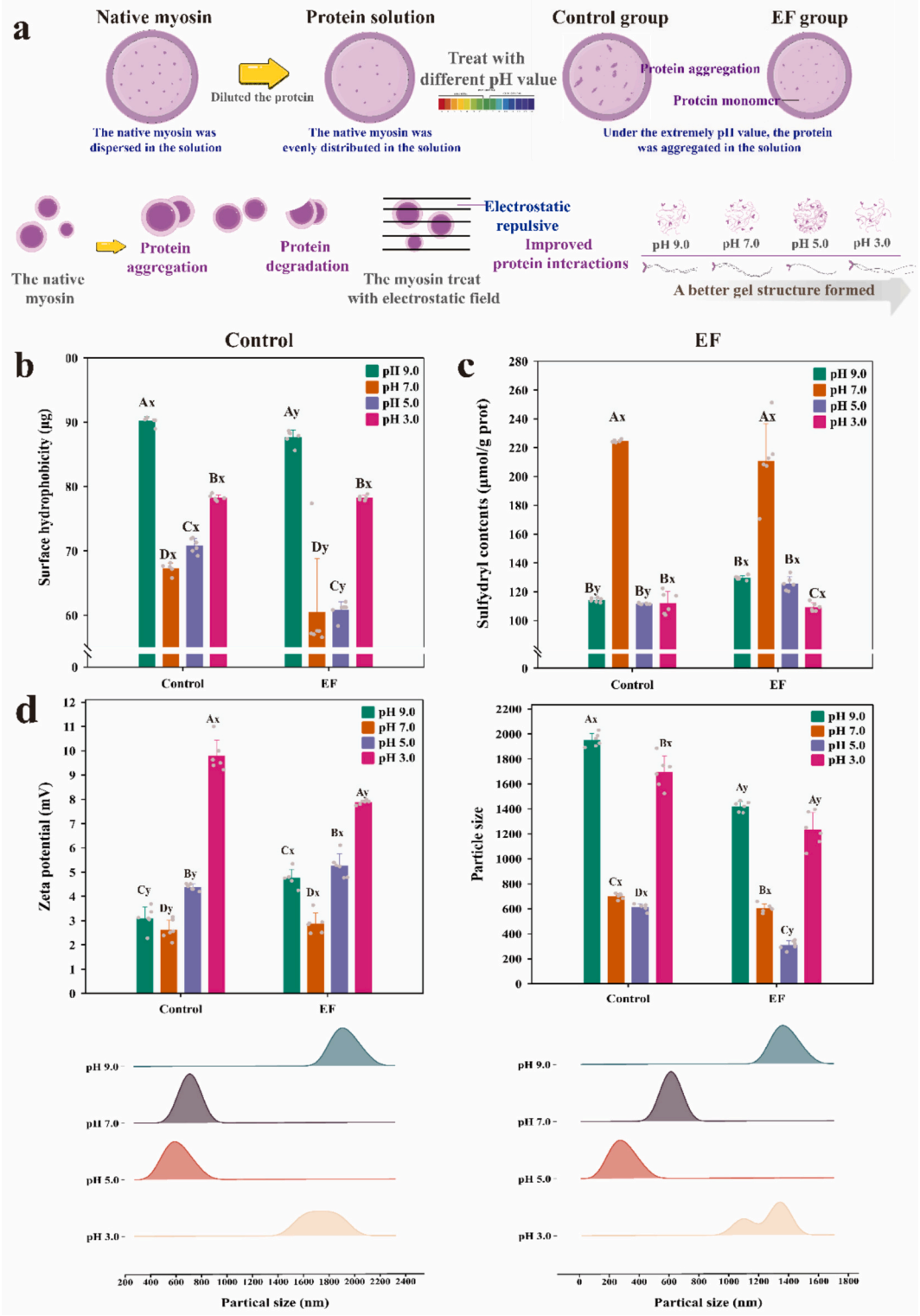

Fig. 1. Effect of electrostatic field treatment on the function of myosin at different pH values. A-D: The significance of the surface hydrophobicity, sulfhydryl group content, Zeta – potential, and particle size at different pH values in the same treatment group ($P < 0.05$). x-y: The significance of surface hydrophobicity, sulfhydryl group content, Zeta – potential, and particle size at the same pH value for different treatment groups ($P < 0.05$). (a): Diagram of MYPs treated by the electrostatic field at different pH values; Diagram of myosin forming a stable gel structure under the application of electrostatic field; (b): Surface hydrophobicity; (c): Sulfhydryl group content; (d): Zeta - potential and particle size.

the cross-linking in protein and allow the new sulfhydryl groups generated without limitation (Chen et al., 2024). Therefore, the degree of protein oxidation was directly correlated with sulfhydryl group content. Yu, Chen, et al. (2024), Yu, Hong, et al. (2024), Yu, Yan, et al. (2024) suggested that a pH environment near the pI leads to a higher sulfhydryl content and a lower protein oxidation degree. Walayat et al. (2024) also concluded consistent with the results. They suggested that sulfhydryl groups undergo deprotonation at extreme pH values to

generate mercaptan compounds, and that the oxidation of sulfhydryl groups was accelerated more quickly in acidic and alkaline conditions. While the higher sulfhydryl group content of MYPs in the electrostatic field indicated that the electrostatic field effectively prevented myosin from degenerating, reduced the exposure of sulfhydryl groups in myosin, and improved the stability of the protein structure, which was in line with the findings of Yang et al. (2024).

3.2. Zeta-potential and particle size of MYPs

As shown in Fig. 1d, obvious Zeta-potential initially decreased and subsequently increased were observed in the two groups. When the pH value was close to the pI (pH 5.5), there was basically no electrostatic repulsion between proteins (Yu et al., 2024). Following treatment with the electrostatic field on MYPs, the exposed groups on the surface were changed completely, with an obvious unbalance between positive

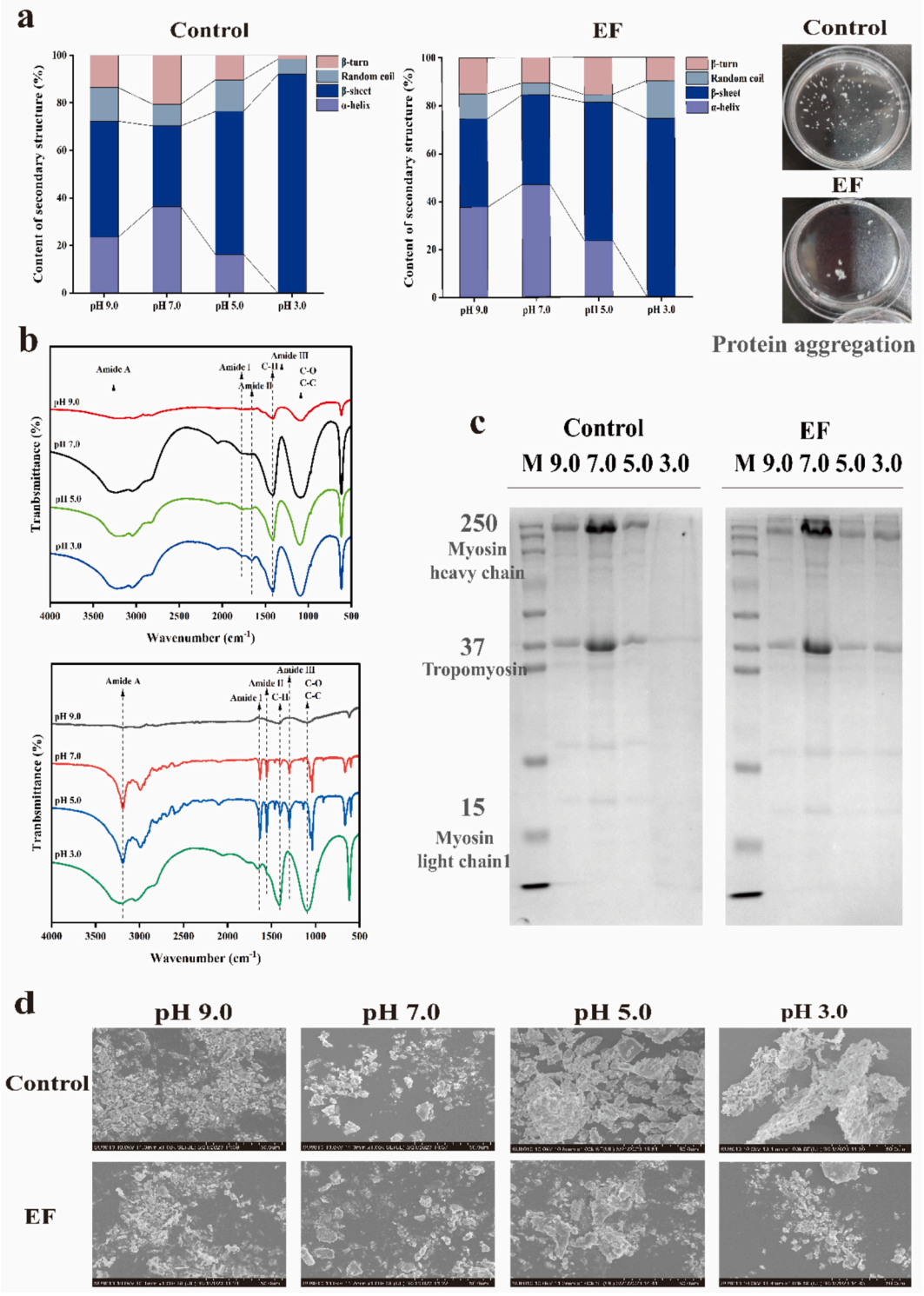

Fig. 2. Effect of electrostatic field treatment on the structure of myosin at different pH values. (a): Secondary structure; (b): Infrared spectroscopy; (c): Scanning electron microscope of microstructure; (d): SDS-PAGE.

charges and negative charges of the protein (Liu et al., 2024). At pH 9.0, 7.0 and 5.0, the Zeta-potential of the EF group was higher than that of the Control group. Hartvig et al. (2011) suggested that the enhancement of electrostatic interactions induces changes in the double electron layer on the protein surface. This might explain why the application of an electrostatic field increases the repulsion between proteins, promoting a more uniform dispersion of myosin in the solution and resulting in a more stable solution system during this phase (Rodrigues et al., 2019). Nevertheless, the presence of a strong acid (pH 3.0) must also be considered, a lower value in the EF group was recorded in Fig. 1d, indicating that the positive charges located on the protein surface that determine the pI, such as NH^{3+}, were insensitive to the influence of the electrostatic field. Therefore, molecules condensed or aggregated due to hydrophobic contact, and the dispersion in solution was inadequate lead to a relative higher value in EF group.

The particle size of MYPs in the Control group decreased from 1949.67 nm to 603.20 nm within pH 9.0–5.0 and increased to 1696.67 nm in pH 3.0, while in the EF group, the particle size was significantly lower than Control group in each point (Fig. 1d). The average particle size of myosin in solution reflects protein aggregation, specifically, the smaller the particle size, the lower the degree of protein aggregation (Chen et al., 2024). According to the acid-base environment of the solution was close to the pI (pH 5.5) of myosin protein (Yu, Chen, et al., 2024; Yu, Hong, et al., 2024; Yu, Yan, et al., 2024), the electrostatic repulsion between myosin molecules was changed, and contributed to the surface hydrophobicity of MYPs dramatically decreased, which was assistant with the result of 3.1. In turn, the electrostatic field provided an increase of electrostatic repulsion of charge between the surface of myosin and resulted in the fracture of ionic bonds (Hartvig et al., 2011). In such a case, the single matrix of myosin could be separated from the polymer, ultimately dictating the average particle size of myosin in solution (Müller et al., 2022). Xie et al. (2013) believe that the coupling of the dipole with the external electrostatic field is mainly due to the position rearrangement of the local atomic charge of the protein. This further supported the limiting effect of the electrostatic field on the conformational change of proteins in solution, consistent with the observation of the Zeta potential.

3.3. Secondary structure of MYPp

As shown in Fig. 2a, in the pH range of 3.0–9.0, the α-helix continuously decreased and the β-sheet significantly increased ($P < 0.05$). The largest percentage of α-helix (36.27 %) and lowest percentage of β-sheet (34.02 %) were found in MYPp at pH 7.0. It was worth noting that the lowest value of α-helix (0 %) and the highest content of β-sheet (92.02 %) were observed at pH 3.0, suggesting that acidic circumstances had a negative effect on the MYPp, which was also in line with the results of (Wen, Mu, et al., 2024; Wen, Zhang, et al., 2024). Similarly, the EF group showed a tendency of decreasing content of α-helix with the pH value decreased from 7.0 to 3.0. The MYPp under electrostatic field exhibited a higher content of α-helix at pH 9.0, 7.0, and 5.0 than the Control group. The changes in α-helix and β-sheet content were attributed to alterations in the number of intramolecular and intermolecular hydrogen bonds in myosin, induced by electrostatic repulsion (Yu, Chen, et al., 2024; Yu, Hong, et al., 2024; Yu, Yan, et al., 2024). This phenomenon was exemplified in the study on surface hydrophobicity. Therefore, it could be speculated that the appearance of an electrostatic field leads to a change in electrostatic repulsion, reduces the enhancement and aggregation of protein-protein cross-linking, and strengthens the bond between the protein and the water molecules (Liu et al., 2024).

Furthermore, the vibration peak of MYPp was analyzed using infrared spectroscopy (Fig. 2b). The amount of tryptophan residues was exposed outside the protein molecule to produce hydrophobic residues as the external environment shifts to acidic and alkaline circumstances, resulting in the hydrophobicity of the protein increased, which was in line with the surface hydrophobicity results. It was possible that the β-sheet structural unfold caused by the electrostatic field allowed the creation of α-helix and promoted hydrogen bonding to possess a decreasing hydrophobicity and a stabilized structure of the protein (Xie et al., 2023).

3.4. SDS-PAGE of MYPs and microstructure of MYPp

As shown in Fig. 2c, the darker the band color, the more stable the protein structure. The degradation of myosin heavy chain, tropomyosin, and myosin light chain 1 and 2 increased at pH 9.0 and 5.0. The bands appeared the shallowest at pH 3.0, suggesting that the protein may have been completely degraded. The protein of the EF group still maintained high activity at different pH values, especially at pH 3.0, the protein bands were more complete than the Control group. Research by Wen, Mu, et al. (2024), Wen, Zhang, et al. (2024) suggested that the extreme pH value breaks the secondary bonds of protein such as ionic bonds, hydrogen bonds, and hydrophobic interaction. Therefore, it could be assumed that the function of intermolecular covalent cross-linking bonds in proteins was weakened at this point, and thus the protein degradation made the bands shallow or disappear. The oxidation of specific protein groups, such as sulfhydryl, methylthioyl, and α-carbon radicals, could alter the charge, conformation, and chemical properties of the protein, ultimately affecting its structure and function (Li et al., 2024). The bands of protein in the EF group were deeper at pH 9.0, 5.0, and 3.0, indicating that the degree of protein oxidation was lower than that in the Control group. The formation of disulfide bonds was reduced and the structure of the protein was stable in the highest and lowest pH value environment.

As shown in Fig. 2d, myosin was close to each other at pH 9.0 due to the enhanced interaction between molecules, and the protein structure was relatively ordered to form a large and fusiform-like protein structure. At pH 7.0, myosin aggregated but distributed evenly, while at pH 5.0, there are a few little protein clumps, most of the proteins exist in the form of small molecules, and the protein particles were small and scattered. When the pH value decreased to 3.0, small molecules formed new, relatively rough and disordered granular aggregates, accompanied by the presence of slightly thick protein filamentous aggregates. The different pH values affected the interaction of tertiary and quaternary structures between the myosin head, leading to internal disulfide bonds and hydrophobic groups were exposed (Fig. 1b). Those large volume proteins were likely to form aggregates with the help of electrostatic repulsion, Van der Waals force and so on, which could be produced by the intermolecular interactions (Yu, Chen, et al., 2024; Yu, Hong, et al., 2024; Yu, Yan, et al., 2024). A few proteins soluble aggregates appeared in the EF group, which was consistent with the results of Hartvig et al. (2011) and Xie et al. (2023). The addition of electrostatic field changes the ionization and static charge values of protein molecules, which promotes the ordering of myosin molecules and makes the solution system more stable.

3.5. Fluorescence spectra of MYPs

The fluorescence intensity of proteins in both groups peaked at pH 5.0 and decreased at pH 3.0, as indicated by Fig. 3a. The tryptophan residues encased in the hydrophobic structure of protein exhibited increased fluorescence intensity upon stimulation when myosin was folded. The results were aligned with the reports of the Yu, Chen, et al. (2024), Yu, Hong, et al. (2024), Yu, Yan, et al. (2024) investigation, and the authors presumed a connection between the alteration in protein structure and the decrease in fluorescence intensity. Reduced fluorescence intensity occurred when tryptophan was exposed to the surface of protein molecules due to partial or complete unfolding of myosin at pH 9.0 and 3.0. In addition, the fluorescence intensity of the EF group was higher than that of the Control group at each pH value. This could be attributed to the electrostatic field shielding the tryptophan residues on the surface of the protein. This further indicated that electrostatic field

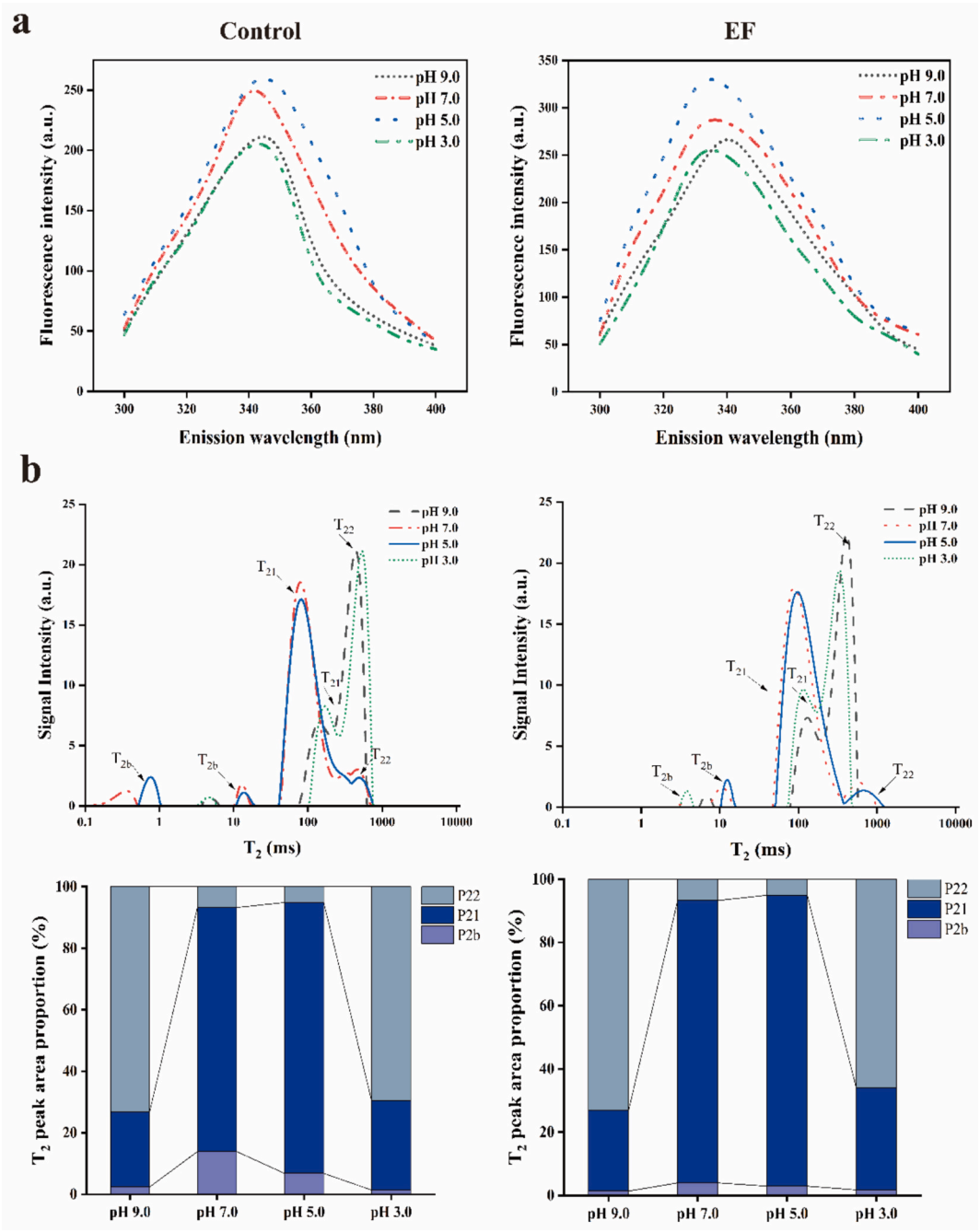

Fig. 3. Effect of electrostatic field treatment on fluorescence intensity of myosin and water holding capacity of myosin gel at different pH values. (a): Fluorescence intensity; (b): T_2 relaxation time.

treatment had a certain delay effect on myosin oxidation, which was also confirmed by the study of Jia et al. (2018), illustrating that the endogenous fluorescence intensity of proteins under electrostatic field was higher.

3.6. The WHC of MYPs gel

The peak area ratio (T_{21}) of immobilized water was the highest at pH 5.0, and the lowest at pH 9.0 and 3.0 (Fig. 3b). This reflected that the immobilized water content decreased mainly because it was difficult for water and macromolecules to combine when MYPs were far from the pI (pH 5.5), resulting in poor WHC of the gel. It has been proposed that the extreme pH value was not conducive to the formation of gels (Sun et al., 2021). When observing the surface of the gel, it was noticed that the texture of the gel was rough and dry at pH 9.0. Furthermore, a significant amount of water escaped from the gel at pH 3.0, confirming that the free water content at pH 3.0 was slightly higher than at pH 9.0. Conversely, the gel structure was dense and uniform at pH 5.0, which was favorable for the maintenance of water molecules. In addition, the content of immobilized was obviously lower than the EF group for gels in the Control group, which could be ascribed to the effect of the electrostatic field on the net charge on the protein surface, leading to the stable water molecules trapped in large cavities in the myosin gel network (Guo et al., 2019). The increase of net charge enhances the hydration and electrostatic interaction between protein and water molecules in MYPs gel and results in a stable network formation (Sun et al., 2021).

The gel image turned purple during the imaging scan at pH 9.0,

suggesting that the water molecules of the Control group were poorly maintained (Fig. 4a). It was suggested that when the protein was close to the pI and the bond between the water molecules and protein was reasonably stable, thus H-proton were better occupied in the image at pH 7.0 and 5.0 (Zhang et al., 2019). In addition, the image exhibited a significant quantity of blue region at pH 3.0, which indicated a significant amount of water was lost since acidic conditions cause changes in the charged groups on the surface of the protein (Liu et al., 2008). As the electrostatic field progressed, the H-proton in gel exhibited an aggregation trend, with intensity continuously increasing and the color changing from yellow to red at pH 7.0–5.0. Additionally, the gel of the EF group was more complete at pH 9.0 and the gel surface of the EF group was less hydrated at pH 3.0.

As illustrated in Fig. 4b, the centrifugal loss of both the Control group and EF group exhibited a decreased trend followed by an increase within the range of pH 9.0–3.0 ($P < 0.05$). The significant changes did not occur until pH 3.0, indicating that the protein has deviated from the pI could achieve a decrease in the static charged group on the protein, which led to the loss of immobilized water and free water (Zhao et al., 2020). EF gels exhibited a lower centrifugal loss at pH 3.0, indicating that a

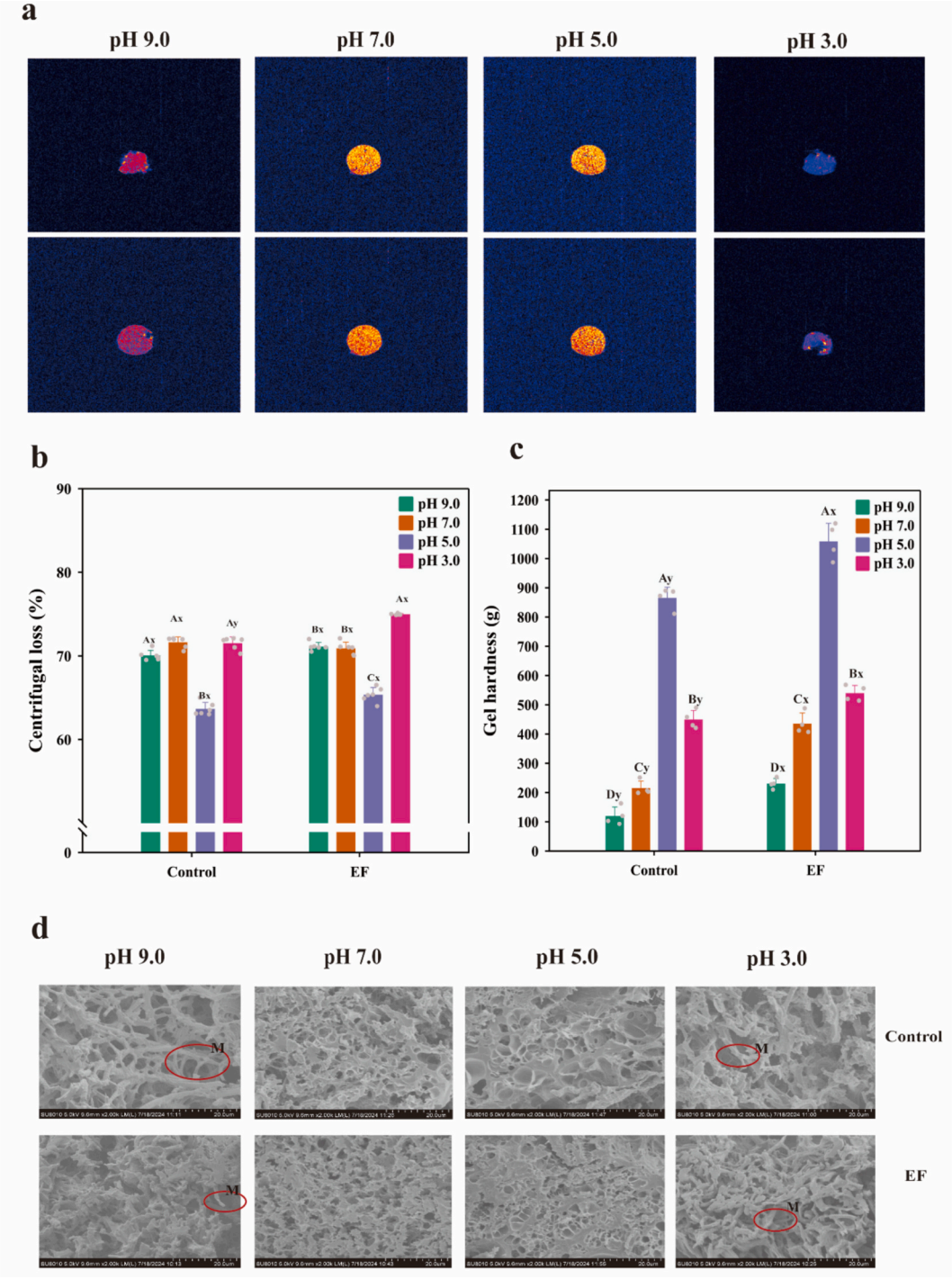

Fig. 4. Effect of electrostatic field treatment on structure water holding capacity and of myosin gel at different pH values. A-D: The significance of the centrifugation loss and hardness at different pH values in the same treatment group ($P < 0.05$). x-y: The significance of centrifugation loss and hardness at the same pH value for different treatment groups ($P < 0.05$). (a): Distribution of H-proton; (b): Centrifugation loss; (c): Hardness; (d): Scanning electron microscope of microstructure.

positive effect might occur on the binding of protein molecules induced by the electrostatic field, thus leading to a well-formed gel (Yu, Chen, et al., 2024; Yu, Hong, et al., 2024; Yu, Yan, et al., 2024). Zhang et al. (2024) believed that the increased hydrogen bonding and net charge could be the main trigger of the enhanced WHC of protein gels. As the net charge increased under the electrostatic field treatment, the protein aggregation decreased, allowing the myosin protein to form a structure that maintained the immobilized water and free water inside the gels.

3.7. The TPA of MYPs gel

The hardness, springiness, gumminess, chewiness, and whiteness involved in texture characteristics were well recognized as the main factors for assessing the gel formation. The altering pH value influences the protein structure, thereby modifying the gel texture characteristics. As shown in Table 1, the gumminess, chewiness, and whiteness were changed insignificantly at pH 9.0–5.0 ($P > 0.05$). At pH 3.0, the protein was under acidic conditions and far away from the pI, the net positive charge of the protein increased significantly. The charge was exposed to the weak electrostatic repulsion, leading to the aggregation and denaturation of protein. It was negative for the protein to form a stable and ordered network, contributing to the variation of gumminess, chewiness, and whiteness.

After the protein was made into a gel, the variation trend of gel hardness at each pH value was decrease of pH value (9.0–3.0), the gel hardness of the gel increased first and then decreased (Fig. 4c). The gel had a highly rough exterior at pH 9.0 and was extensively fractured following determination, while the look of gel was comparatively smooth at pH 5.0. The increase of gel hardness may be due to the stable maintenance of immobilized water in the network of gel caused by the decreased degree of protein degradation. The result was in agreement with Liu et al. (2010) who suggested the effect on the gel properties of protein, with the decrease of pH value, the gelation rate and gel hardness of protein increased in the range of pH 9.0–5.5. The gel hardness dropped once more when the pH value dropped to 3.0, and a significant amount of water appeared on the gel surface, likely because of a significant loss of free water. The variation trend of the EF group was similar to the Control group, while the gel hardness was significantly higher than that of the Control group, meanwhile, relatively a smoother appearance of the gel surface was observed. The appearance of an electrostatic field moderately enhanced the number and intensity of charge on protein, thereby increasing the binding of protein to protein and protein to water molecule (Wen, Mu, et al., 2024; Wen, Zhang, et al., 2024). It was conducive to forming a dense and uniform gel structure, resulting in improved gel hardness.

Table 1
Effect of electrostatic field on texture properties of myosin gels at different pH values A-D: The significance of the springiness, gumminess, chewiness, and whiteness at different pH values in the same treatment group ($P < 0.05$). x-y: The significance of springiness, gumminess, chewiness, and whiteness at the same pH value for different treatment groups ($P < 0.05$).

pH	Treatment	Springiness	Gumminess	Chewiness	Whiteness
9.0	Control	0.413 ± 0.003^{Bx}	0.436 ± 0.001^{Bx}	18.26 ± 0.08^{Cx}	62.78 ± 0.11^{Dx}
	EF	0.437 ± 0.005^{Bx}	0.439 ± 0.018^{Bx}	19.00 ± 0.03^{Cx}	60.77 ± 0.14^{Cx}
7.0	Control	0.667 ± 0.007^{Ax}	0.519 ± 0.008^{Ax}	59.04 ± 0.09^{Ax}	71.81 ± 0.17^{Bx}
	EF	0.687 ± 0.007^{Ax}	0.521 ± 0.002^{Ax}	57.99 ± 0.04^{Ax}	70.57 ± 0.16^{Bx}
5.0	Control	0.328 ± 0.011^{Cx}	0.291 ± 0.002^{Cx}	41.72 ± 0.09^{Bx}	90.51 ± 0.16^{Ax}
	EF	0.360 ± 0.004^{Cx}	0.288 ± 0.002^{Cx}	41.49 ± 0.13^{Bx}	88.91 ± 0.10^{Ax}
3.0	Control	0.255 ± 0.001^{Dx}	0.172 ± 0.001^{Dy}	16.45 ± 0.16^{Dx}	67.92 ± 0.09^{Cx}
	EF	0.245 ± 0.003^{Dx}	0.239 ± 0.001^{Cx}	12.62 ± 0.13^{Dy}	52.63 ± 0.11^{Dy}

3.8. The microstructure of MYPs gel

The SEM in the gel structure was shown in Fig. 4d. The cross-linking between protein gel networks was weak at pH 9.0, and the many aggregates of varying sizes were interlaced with each other. At pH 7.0–5.0, which is near the pI of protein, the gel formed a relatively ordered, high density and small and uniform pore size gel network structure. At pH 3.0, the gel micelles appear rough and irregularly shaped, while the gel pore size was large and uneven. Slightly thick protein filamentous aggregates around the pores could be observed within the microstructure, and it is worth noting that there were several rod-shaped or spherical protein particles at the M position. The dense protein structure could be observed in neutral conditions, while the presence of extreme pH value might be more effective than neutral in influencing the electrostatic interaction between myosin molecules, which is also proved by Yu, Chen, et al. (2024), Yu, Hong, et al. (2024), Yu, Yan, et al. (2024). Noticeably, the gels in EF group had a relatively flat structure at pH 9.0–5.0, which could account for the higher WHC in in the structure. Even though some visible uneven pores appeared on the surface at pH 3.0, possibly due to the minimal net surface charge on the proteins caused by an electrostatic field, thus reducing the aggregation of filamentous polymer (Zhang et al., 2024). This caused the myosin molecules to occupy more space within the gel to form an ordered three-dimensional network structure, further supporting the theory that the electrostatic field protects the molecular structure of the protein.

4. Conclusion

The electrostatic field had a major impact on the structure and function of myosin at various pH values. The results of surface hydrophobicity and sulfhydryl group content demonstrated that the process of oxidative denaturation of myosin could be delayed by the electrostatic field at pH 9.0 and 3.0. As indicated by the results of particle size and Zeta-potential, secondary structure, microstructure changes, and protein degradation, the electrostatic field could enhance the electrostatic interaction between proteins by releasing electric charges, thereby improving the structural and functional characteristics of proteins damaged by the highest and lowest pH value. The findings of T_2 relaxation and centrifugal loss of myosin gel demonstrated that the electrostatic field decreased the amount of immobilized water that was transferred to free water, leading to a reduced moisture loss, which proved that the electrostatic field enhanced the connection between the protein and the water molecule. As evidenced by the hardness analysis and SEM results of the myosin gel, a stronger and dense structure formed by the myosin gel could be encouraged by the electrostatic field, which would help to better maintain the water molecule in the gel. Therefore, it could be concluded that the electrostatic field protects the structure and function of myosin at different pH values. This may be beneficial to the future explanation of the mechanism of enhancing muscle quality in the electrostatic field.

CRediT authorship contribution statement

Yuqian Xu: Writing – review & editing, Writing – original draft, Software, Resources, Investigation, Formal analysis, Data curation, Conceptualization. **Dongmei Leng:** Visualization, Supervision, Investigation, Data curation, Conceptualization. **Martine Schroyen:** Writing – review & editing, Visualization, Resources, Methodology, Investigation, Formal analysis. **Xin Li:** Writing – review & editing, Supervision, Software, Formal analysis, Conceptualization. **Debao Wang:** Writing – review & editing, Software, Methodology, Investigation, Conceptualization. **Dequan Zhang:** Writing – review & editing, Supervision, Resources, Funding acquisition, Conceptualization. **Chengli Hou:** Writing – review & editing, Supervision, Software, Investigation,

Funding acquisition, Formal analysis.

Declaration of competing interest

The authors confirm that there are no conflicts of interest.

Data availability

Data will be made available on request.

Acknowledgements

This work was supported by the Key R&D Program of Shandong Province, China (2023CXGC010708). The authors appreciate the assistance by Mrs. Yanli Sun and Mrs. Ying Wang of the Electron Microscope Center and Mrs. Chunhong Li and Lan Tian of the National Key Laboratory of Argo-products Processing, Institute of Food Science and Technology, Chinese Academy of Agricultural Sciences.

References

Chen, C., Liu, Z., Xiong, W., Yao, Y., Li, J., & Wang, L. (2024). Effect of alkaline treatment duration on rapeseed protein during pH-shift process: Unveiling physicochemical properties and enhanced emulsifying performance. *Food Chemistry, 459*, Article 140280. https://doi.org/10.1016/j.foodchem.2024.140280

Chen, H., Zou, Y., Zhou, A., Liu, X., & Benjakul, S. (2023). Elucidating the molecular mechanism of water migration in myosin gels of *Nemipterus virgatus* during low pressure coupled with heat treatment. *International Journal of Biological Macromolecules, 253*, Article 126815. https://doi.org/10.1016/j.ijbiomac.2023.126815

Deng, Y., Wang, R., Xu, M., Li, X., Zhang, Y., Gooneratne, R., & Li, J. (2025). Elucidating the binding mechanism of silver carp myosin to T-2 toxin using multi-spectroscopic analysis, molecular docking and molecular dynamics simulation. *LWT, 117532*. https://doi.org/10.1016/j.lwt.2025.117532

Guo, Z., Li, Z., Wang, J., & Zheng, B. (2019). Gelation properties and thermal gelling mechanism of golden threadfin bream myosin containing $CaCl_2$ induced by high pressure processing. *Food Hydrocolloids, 95*, 43–52. https://doi.org/10.1016/j.foodhyd.2019.04.017

Han, G., Li, Y., Liu, Q., Chen, Q., Liu, H., & Kong, B. (2022). Improved water solubility of myofibrillar proteins by ultrasound combined with glycation: A study of myosin molecular behavior. *Ultrasonics Sonochemistry, 89*, Article 106140. https://doi.org/10.1016/j.ultsonch.2022.106140

Hartvig, R. A., van de Weert, M., Østergaard, J., Jorgensen, L., & Jensen, H. (2011). Protein adsorption at charged surfaces: The role of electrostatic interactions and interfacial charge regulation. *Langmuir, 27*(6), 2634–2643. https://doi.org/10.1021/la104720n

Jia, G., Nirasawa, S., Ji, X., Luo, Y., & Liu, H. (2018). Physicochemical changes in myofibrillar proteins extracted from pork tenderloin thawed by a high-voltage electrostatic field. *Food Chemistry, 240*, 910–916. https://doi.org/10.1016/j.foodchem.2017.07.138

Li, S., Zhang, K., Wu, Y., Chen, Q., Li, M., Kong, B., & Zhang, C. (2024). Role of ultrasonic freezing-treated pork dumpling filling during frozen storage: Insights from protein oxidation, aggregation, and functional properties. *International Journal of Refrigeration, 165*, 223–232. https://doi.org/10.1016/j.ijrefrig.2024.05.035

Lin, H., Wang, J., Chisoro, P., Wu, G., Zhao, S., Hu, X., Yang, C., Liu, Y., Jia, W., Li, Q., Zhang, C., Blecker, C., & Li, X. (2025). Changes in freezing parameters and temperature distribution of beef induced by AC electric field: Alleviation on freezing damage and myowater loss. *Journal of Food Engineering, 387*, Article 112343. https://doi.org/10.1016/j.jfoodeng.2024.112343

Liu, M., Wei, Y., Li, X., Quek, S. Y., Zhao, J., Zhong, H., … Liu, Y. (2018). Quantitative phosphoproteomic analysis of caprine muscle with high and low meat quality. *Meat Science, 141*, 103–111. https://doi.org/10.1016/j.meatsci.2018.01.001

Liu, P., Hou, M., Yue, Y., Tong, Y., Zhang, T., Lu, Z., & Yang, L. (2023). Effects of ultrahigh magnetic field on the structure and properties of whey protein. *LWT, 177*, Article 114590. https://doi.org/10.1016/j.lwt.2023.114590

Liu, Q., Yang, Q., Wang, Y., Jiang, Y., & Chen, H. (2024). Pretreatment with low-frequency magnetic fields can improve the functional properties of pea globulin amyloid-like fibrils. *Food Chemistry, 439*, Article 138135. https://doi.org/10.1016/j.foodchem.2023.138135

Liu, R., Zhao, S., Liu, Y., Yang, H., Xiong, S., Xie, B., & Qin, L. (2010). Effect of pH on the gel properties and secondary structure of fish myosin. *Food Chemistry, 121*(1), 196–202. https://doi.org/10.1016/j.foodchem.2009.12.030

Liu, R., Zhao, S., Xiong, S., Xie, B., & Qin, L. (2008). Role of secondary structures in the gelation of porcine myosin at different pH values. *Meat Science, 80*(3), 632–639. https://doi.org/10.1016/j.meatsci.2008.02.014

Liu, Y.-F., Oey, I., Bremer, P., Silcock, P., & Carne, A. (2018). Proteolytic pattern, protein breakdown and peptide production of ovomucin-depleted egg white processed with heat or pulsed electric fields at different pH. *Food Research International, 108*, 465–474. https://doi.org/10.1016/j.foodres.2018.03.075

Müller, W. A., Sarkis, J. R., Marczak, L. D. F., & Muniz, A. R. (2022). Molecular dynamics study of the effects of static and oscillating electric fields in ovalbumin. *Innovative Food Science & Emerging Technologies, 75*, Article 102911. https://doi.org/10.1016/j.ifset.2021.102911

Pereira, R. N., Rodrigues, R., Avelar, Z., Leite, A. C., Leal, R., Pereira, R. S., & Vicente, A. (2024). Electrical fields in the processing of protein-based foods. *Foods, 13*(4), 4. https://doi.org/10.3390/foods13040577

Qian, S., Li, X., Wang, H., Mehmood, W., Zhong, M., Zhang, C., & Blecker, C. (2019). Effects of low voltage electrostatic field thawing on the changes in physicochemical properties of myofibrillar proteins of bovine *longissimus dorsi* muscle. *Journal of Food Engineering, 261*, 140–149. https://doi.org/10.1016/j.jfoodeng.2019.06.013

Rodrigues, R. M., Avelar, Z., Machado, L., Pereira, R. N., & Vicente, A. A. (2020). Electric field effects on proteins – Novel perspectives on food and potential health implications. *Food Research International, 137*, Article 109709. https://doi.org/10.1016/j.foodres.2020.109709

Rodrigues, R. M., Vicente, A. A., Petersen, S. B., & Pereira, R. N. (2019). Electric field effects on β-lactoglobulin thermal unfolding as a function of pH – Impact on protein functionality. *Innovative Food Science & Emerging Technologies, 52*, 1–7. https://doi.org/10.1016/j.ifset.2018.11.010

Sun, H., Zhang, Y., & Sun, J. (2024). Dietary inulin supplementation improves the physicochemical and gel properties of duck myofibrillar protein: Insights into the effect of muscle fiber types. *Food Hydrocolloids, 150*, Article 109722. https://doi.org/10.1016/j.foodhyd.2023.109722

Sun, Y., Ma, L., Fu, Y., Dai, H., & Zhang, Y. (2021). The improvement of gel and physicochemical properties of porcine myosin under low salt concentrations by pulsed ultrasound treatment and its mechanism. *Food Research International, 141*, Article 110056. https://doi.org/10.1016/j.foodres.2020.110056

Walayat, N., Wei, R., Su, Z., Lorenzo, J. M., & Nawaz, A. (2024). Effect of tea polysaccharides on fluctuated frozen storage impaired total sulfhydryl level and structural attributes of silver carp surimi proteins. *Food Hydrocolloids, 157*, Article 110448. https://doi.org/10.1016/j.foodhyd.2024.110448

Walayat, N., Xiong, Z., Xiong, H., Moreno, H. M., Niaz, N., Ahmad, M. N., … Wang, P.-K. (2020). Cryoprotective effect of egg white proteins and xylooligosaccharides mixture on oxidative and structural changes in myofibrillar proteins of *Culter alburnus* during frozen storage. *International Journal of Biological Macromolecules, 158*, 865–874. https://doi.org/10.1016/j.ijbiomac.2020.04.093

Wang, Q., Li, Y., Sun, D.-W., & Zhu, Z. (2018). Enhancing food processing by pulsed and high voltage electric fields: Principles and applications. *Critical Reviews in Food Science and Nutrition, 58*(13), 2285–2298. https://doi.org/10.1080/10408398.2018.1434609

Wang, W., Lin, H., Guan, W., Song, Y., He, X., & Zhang, D. (2024). Effect of static magnetic field-assisted thawing on the quality, water status, and myofibrillar protein characteristics of frozen beef steaks. *Food Chemistry, 436*, Article 137709. https://doi.org/10.1016/j.foodchem.2023.137709

Wen, H., Zhang, D., Ning, Z., Li, Z., Zhang, Y., Liu, J., Yu, T., & Zhang, T. (2024). Effect of benzoic acid-based and cinnamic acid-based polyphenols on foaming properties of ovalbumin at acidic, neutral and alkaline pH conditions. *Food Hydrocolloids, 153*, Article 109998. https://doi.org/10.1016/j.foodhyd.2024.109998

Wen, X., Mu, Z., Gantumur, M.-A., Bilawal, A., Jiang, Z., & Zhang, L. (2024). Characterization of whey protein isolate aggregation induced by different acidic substances: Triggered by disulfide bond formation and recombination. *Food Hydrocolloids, 157*, Article 110414. https://doi.org/10.1016/j.foodhyd.2024.110414

Xie, Y., Chen, B., Guo, J., Nie, W., Zhou, H., Li, P., Zhou, K., & Xu, B. (2021). Effects of low voltage electrostatic field on the microstructural damage and protein structural changes in prepared beef steak during the freezing process. *Meat Science, 179*, Article 108527. https://doi.org/10.1016/j.meatsci.2021.108527

Xie, Y., Liao, C., & Zhou, J. (2013). Effects of external electric fields on lysozyme adsorption by molecular dynamics simulations. *Biophysical Chemistry, 179*, 26–34. https://doi.org/10.1016/j.bpc.2013.05.002

Xie, Y., Zhou, K., Chen, B., Ma, Y., Tang, C., Li, P., Wang, Z., Xu, F., Li, C., Zhou, H., & Xu, B. (2023). Mechanism of low-voltage electrostatic fields on the water-holding capacity in frozen beef steak: Insights from myofilament lattice arrays. *Food Chemistry, 428*, Article 136786. https://doi.org/10.1016/j.foodchem.2023.136786

Xie, Y., Zhou, K., Chen, B., Wang, Y., Nie, W., Wu, S., Wang, W., Li, P., & Xu, B. (2021). Applying low voltage electrostatic field in the freezing process of beef steak reduced the loss of juiciness and textural properties. *Innovative Food Science & Emerging Technologies, 68*, Article 102600. https://doi.org/10.1016/j.ifset.2021.102600

Xu, Y., Leng, D., Li, X., Wang, D., Chai, X., Schroyen, M., Zhang, D., & Hou, C. (2024). Effects of different electrostatic field intensities assisted controlled freezing point storage on water holding capacity of fresh meat during the early postmortem period. *Food Chemistry, 439*, Article 138096. https://doi.org/10.1016/j.foodchem.2023.138096

Xu, Y., Zhang, D., Xie, F., Li, X., Schroyen, M., Chen, L., & Hou, C. (2023). Changes in water holding capacity of chilled fresh pork in controlled freezing-point storage assisted by different modes of electrostatic field action. *Meat Science, 204*, Article 109269. https://doi.org/10.1016/j.meatsci.2023.109269

Yang, C., Wu, G., Liu, Y., Li, Y., Zhang, C., Liu, C., & Li, X. (2024). Low-voltage electrostatic field enhances the frozen force of −12°C to suppress oxidative denaturation of the lamb protein during the subsequent frozen storage process after finishing initial freezing. *Food Chemistry, 438*, Article 138055. https://doi.org/10.1016/j.foodchem.2023.138055

Yu, C., Chen, L., Xu, M., Ouyang, K., Chen, H., Lin, S., & Wang, W. (2024). The effect of pH and heating on the aggregation behavior and gel properties of beef myosin. *LWT, 191*, Article 115615. https://doi.org/10.1016/j.lwt.2023.115615

Yu, Q., Hong, H., Liu, Y., Monto, A. R., Gao, R., & Bao, Y. (2024). Oxidation affects pH buffering capacity of myofibrillar proteins via modification of histidine residue and structure of myofibrillar proteins. *International Journal of Biological Macromolecules, 260*, Article 129532. https://doi.org/10.1016/j.ijbiomac.2024.129532

Yu, S., Yan, J.-K., Jin, M.-Y., Li, L.-Q., Yu, Y.-H., & Xu, L. (2024). Preparation, physicochemical and functional characterization of pectic polysaccharides from fresh passion fruit peel by magnetic-induced electric field-assisted three-phase partitioning. *Food Hydrocolloids, 156*, Article 110292. https://doi.org/10.1016/j.foodhyd.2024.110292

Zhang, A., Chen, S., Wang, Y., Zhou, G., Wang, L., Wang, X., & Xu, N. (2019). Effect of different homogenization pressure on soy protein isolate-vitamin D3 complex. *Process Biochemistry, 87*, 145–150. https://doi.org/10.1016/j.procbio.2019.09.011

Zhang, Y., Lyu, H., Wang, Y., Bai, G., Wang, J., Teng, W., Wang, W., & Cao, J. (2024). Optimizing the formation of myosin/high-density lipoprotein composite gels: PH-dependent effects on heat-induced aggregation. *International Journal of Biological Macromolecules, 268*, Article 131786. https://doi.org/10.1016/j.ijbiomac.2024.131786

Zhao, X., Han, G., Sun, Q., Liu, H., Liu, Q., & Kong, B. (2020). Influence of lard-based diacylglycerol on the rheological and physicochemical properties of thermally induced pork myofibrillar protein gels at different pH levels. *LWT, 117*, Article 108708. https://doi.org/10.1016/j.lwt.2019.108708

Zhou, F., Zhao, M., Cui, C., & Sun, W. (2015). Influence of linoleic acid-induced oxidative modifications on physicochemical changes and in vitro digestibility of porcine myofibrillar proteins. *LWT, 61*(2), 414–421. https://doi.org/10.1016/j.lwt.2014.12.037

Zhou, Y., & Yang, H. (2020). Enhancing tilapia fish myosin solubility using proline in low ionic strength solution. *Food Chemistry, 320*, Article 126665. https://doi.org/10.1016/j.foodchem.2020.126665